

Microsyst Technol (2014) 20:291–302
DOI 10.1007/s00542-013-1863-3

TECHNICAL PAPER

Modeling the instability of CNT tweezers using a continuum model

Amin Farrokhbabadi · Ali Koochi ·
Mohamadreza Abadyan

Received: 8 February 2013 / Accepted: 12 June 2013 / Published online: 25 June 2013
© Springer-Verlag Berlin Heidelberg 2013

Abstract Carbon nanotube (CNT) tweezers are composed of two parallel cantilever CNTs with a distance in between. In this paper, the static response and instability of CNT-made nano-tweezers is theoretically investigated considering the effects of Coulomb electrostatic force and van der Waals molecular attraction. For this purpose, a nano-scale continuum model is employed to obtain the nonlinear constitutive equation of the nano-tweezers. The Euler–Bernoulli beam theory is applied to model the elastic response of the CNT. The van der Waals attraction is computed from the simplified Lennard-Jones potential. In order to solve the nonlinear constitutive equation of the system, three approaches, e.g. the homotopy perturbation method (HPM), the Adomian decomposition (AD) and the finite difference method (FDM) are employed. The obtained results are in good agreement with the experimental measurements. As a case study, freestanding CNT tweezers has been investigated and the detachment length and minimum initial gap of the tweezers are determined. Moreover, the effective operation range of the van der Waals attraction that affects the instability behavior of the CNT tweezers is discussed.

1 Introduction

In recent years carbon nano-tube (CNT) has been widely used in developing advanced materials and ultra-small devices. This is the result of excellent physical characteristics of this material i.e. high aspect ratio, flexibility, and conductivity. CNT are utilized in developing many nano-electromechanical systems (NEMS) such as resonators (Sazonova et al. 2004), relays (Kinaret et al. 2003; Lee et al. 2004), switches (Baughman et al. 1999; Zarei and Rezazadeh 2008) and tweezers (Desquesnes et al. 2002; Akita and Nakayama 2002; Sasaki et al. 2006). CNT-made nano-tweezers are composed of two parallel cantilever CNT electrodes (arms) with a distance in between. Applying a voltage differential between the two arms, they approach each other due to the presence of electrostatic Coulomb forces. The tips of the arms move closer together similar to conventional tweezers and can be used to manipulate nano-scale objects. At a critical voltage, which is known as the pull-in instability voltage, the CNT electrodes become unstable and attach to one another. This critical voltage limits the range of stable displacement of the arms, which is known as the tweezing range and consequently the size of objects that can be manipulated by the nano-tweezers. Therefore predicting the stable tweezing range and the pull-in instability parameters are important issues for designing reliable nano-devices.

In order to investigate the electromechanical behavior of CNT-based nanostructures, several approaches have been employed in the literature. Molecular mechanics/dynamics simulation is one of the more common approaches, which are used to study the CNT/graphene interaction (Sasaki et al. 2006). Sasaki et al. (2006) applied this approach to simulate the peeling of CNT laminations from the graphite substrate and showed that the results of a linear model

A. Farrokhbabadi
Department of Aerospace Engineering, Semnan University,
Semnan, Iran
e-mail: amin.farrokh@profs.semnan.ac.ir

A. Koochi
Department of Engineering, Shahrekord branch,
Islamic Azad University, Shahrekord, Iran

M. Abadyan (✉)
Shahrekord University of Medical Sciences, Shahrekord, Iran
e-mail: abadyan@yahoo.com

closely match the experimental data. However, molecular mechanics/dynamics is a very time-consuming procedure for engineering simulations and might not be easily adapted for investigating nanostructures with a large number of atoms. An alternative simpler approach to study the instability of nanostructures is applying lumped parameter models (Desquesnes et al. 2002; Lin and Zhao 2005; Lee and Kim 2005). Strus et al. (2008) applied a semi-lumped parameter model to investigate the physics of the peeling of CNT laminations from different substrates.

Although lumped parameter models can simply explain the physical behavior of a nanostructure, the precision of such results is not very reliable. An alternative, reliable approach to nano-scale simulation is applying nano-scale continuum models (Ke et al. 2005; Jiang et al. 2007; Koochi et al. (2011a, b). Lee and Kim (2005) applied a continuum model to investigate the deflection of nano-tweezers. Wang et al. (2004) studied the stability of nano-tweezers using a continuum model by employing the Galerkin method. They have studied the static pull-in conditions of freestanding arms taking the van der Waals force into account. However, they have not considered the electrostatic force in their model. In another research, Ramezani (2011) investigated the pull-in behavior of beam-plate type nano-tweezers with square cross-section arms using a continuum model.

In present study, the static behavior of CNT-based nano-tweezers is investigated using a continuum mechanics approach. The effects of electrical and van der Waals forces on the pull-in behavior of the nano-tweezers are considered in the developed model. The elastic response of the system is modeled using Euler–Bernoulli beam theory. Although continuum models provide more accurate results than the lumped models, this approach often leads to highly nonlinear constitutive equations that cannot be solved analytically. In order to solve the nonlinear equation of nano-systems, numerical method (Ma et al. 2010) or analytical methods such as Adomian decomposition (Duan et al. 2013; Soroush et al. 2010), homotopy analysis (Mojahedi et al. 2011) and homotopy perturbation (Abadyan et al. 2011; Moeenfard et al. 2011; Koochi et al. 2011c) can be applied. In this work, three approaches e.g. the homotopy perturbation method (HPM), the Adomian decomposition (AD) and the finite differential method (FDM) is employed to solve the nonlinear constitutive equation of the nano-tweezers. The obtained results are verified by comparing with experimental measurements from literature.

2 Theoretical model

Figure 1a shows the SEM photo of a typical CNT-based nano-tweezers composed of two parallel cantilevers CNT

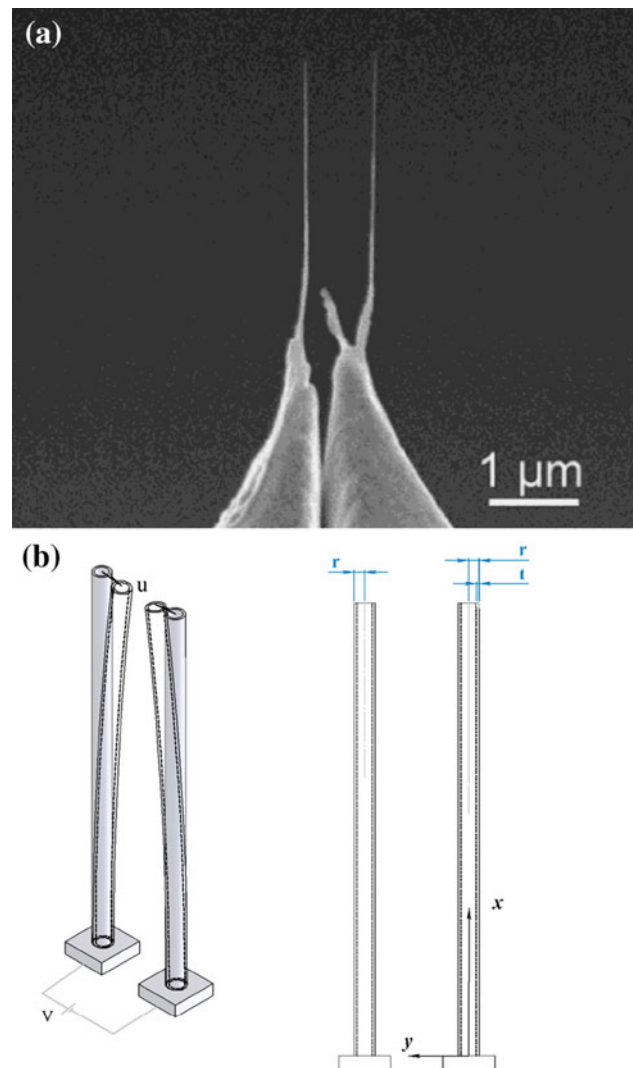


Fig. 1 a SEM photo of typical CNT tweezers. b Schematic configuration of nano-tweezers and the geometrical parameters

arms (Akita and Nakayama 2002). For developing a theoretical model, consider the CNT arms have length L , outer radius of r and effective thickness of t (see Fig. 1b for schematic representation). The initial distance between the two CNTs is g . The CNT arms deflect toward each other due to the presence of electrostatic and van der Waals forces which would be considered in characteristic equation of CNT-based tweezers.

2.1 Electrostatic Coulomb force

The electrostatic forces are computed by using a standard capacitance model (Jackson 1998). The nano-tube is considered as a perfect cylindrical conductor. The capacitance per unit length for two parallel cylindrical beams that are oppositely charged is given by (Hayt 1981):

$$C(g) = \frac{2\pi\epsilon_0}{\ln\left[1 + \frac{g}{r} + \sqrt{\left(\frac{g}{r} + 1\right)^2 - 1}\right]} \tag{1}$$

where ϵ_0 is the permittivity of vacuum. Therefore, the electrostatic energy per unit length is given by:

$$E_{elec} = \frac{1}{2}C(g)V^2 = \frac{\pi\epsilon_0V^2}{\ln\left[1 + \frac{g}{r} + \sqrt{\left(\frac{g}{r} + 1\right)^2 - 1}\right]} \tag{2}$$

Now the electrostatic force per unit length, f_{elec} , can be obtained from (2) as:

$$f_{elec} = \frac{dE_{elec}}{dg} = \frac{\epsilon_0\pi V^2}{\sqrt{g^2 + 2gr} \times \left[\ln\left(1 + \frac{g}{r} + \frac{g}{r}\sqrt{1 + \frac{2r}{g}}\right)\right]^2} \tag{3}$$

where V is the applied voltage and U_1 and U_2 is the deflection of CNTs. It should be noted that by applying the external voltage on the nano-tweezers, the CNTs will deflect to each other to reduce their between gaps from g to $g-U_1-U_2$. If both CNTs have the same geometry and material properties, their deflections will be equal ($U_1 = U_2 = U$). Thus by replacing g with $g-2U$ in relation (3) we have:

$$f_{elec} = \frac{\epsilon_0\pi V^2}{\sqrt{(g-2U)^2 + 2r(g-2U)} \times \left[\ln\left(1 + \frac{g-2U}{r} + \frac{g-2U}{r}\sqrt{1 + \frac{2r}{g-2U}}\right)\right]^2} \tag{4}$$

Using the Taylor series expansion, the above relation can be written as:

$$f_{elec} = \frac{\epsilon_0\pi V^2}{(g-2U+r) \times \left[\ln\left(\frac{2}{r}(r+g-2U)\right)\right]^2} \tag{5}$$

It is worth noting that, the diameter of tubes (r) is much less than the distance between nanotweezers, g , i.e. $r \ll g$. Therefore, the electrical force can be rewritten as:

$$f_{elec} = \frac{\epsilon_0\pi V^2}{g\left(1 - \frac{2U}{g}\right) \times \left[\ln\left(\frac{2g}{r}\left(1 - \frac{2U}{g}\right)\right)\right]^2} \tag{6}$$

2.2 van der Waals attraction

The Lennard-Jones potential is a suitable model to describe van der Waals interaction between bodies (Lennard-Jones 1930). It defines the potential between atoms i and j by:

$$\phi_{ij} = \frac{C_{12}}{r_{ij}^{12}} - \frac{C_6}{r_{ij}^6} \tag{7}$$

where r_{ij} is the distance between atoms i and j while C_6 and C_{12} are the attractive and repulsive constants, respectively. For distances higher than 3.4 Å, such as in this paper, the repulsive term decays extremely fast and can be neglected (Desquesnes et al. 2002). For the carbon-carbon interaction, $C_6 = 15.2 \text{ eV}\text{\AA}^6$ (Girifalco et al. 2000). A reliable continuum model has been established to compute the van der Waals energy by double-volume integral of Lennard-Jones potential (Israelachvili 1985; Ke and Espinosa 2006), that is

$$E_{vdW} = \int_{v_1} \int_{v_2} n_1 n_2 \left(-\frac{C_6}{r^6(v_1, v_2)}\right) dv_1 dv_2 = \frac{\bar{A}L}{12\sqrt{2}} \left[\frac{\left(\frac{r_1}{2}\right)^{\frac{1}{2}}}{(g+2t)^{3/2}} + \frac{2\left(\frac{r_1 r_2}{r_1+r_2}\right)^{\frac{1}{2}}}{(g+t)^{3/2}} - \frac{\left(\frac{r_2}{2}\right)^{\frac{1}{2}}}{g^{3/2}}\right] \tag{8}$$

where v_1 and v_2 represent the two domains of integration, and n_1 and n_2 are the densities of atoms in these domains, respectively. The distance between any two points on v_1 and v_2 is $r(v_1, v_2)$. In above relation \bar{A} is the Hamaker constant, r_1 and r_2 are the internal and external radius of CNT arms, respectively.

Now the molecular force per unit length, f_{vdW} , can be obtained from (8) as:

$$f_{vdW} = \frac{dE_{vdW}}{dg} = \frac{\bar{A}}{8\sqrt{2}} \left[\frac{1}{g^{5/2}} \left(\frac{r_2}{2}\right)^{1/2} - \frac{2}{(g+t)^{5/2}} \left(\frac{r_2 r_1}{r_2+r_1}\right)^{1/2} - \frac{1}{(g+2t)^{5/2}} \left(\frac{r_1}{2}\right)^{1/2}\right] \tag{9}$$

It should be noted that by deflecting the arms their between gaps reduce from g to $g-U_1-U_2$. By assuming the similarity of arms and equal geometry for two nano-tubes, the displacements of U_1, U_2 will be the same ($U_1 = U_2 = U$). Therefore, similar to what mentioned about the electrical force, the van der Waals force is derived from Eq. (9) by replacing g with $g-2U$:

$$f_{vdW} = \frac{\bar{A}}{8\sqrt{2}} \left[\frac{1}{(g-2U)^{5/2}} \left(\frac{r_2}{2}\right)^{1/2} - \frac{2}{(g+t-2U)^{5/2}} \times \left(\frac{r_2 r_1}{r_2+r_1}\right)^{1/2} - \frac{1}{(g+2t-2U)^{5/2}} \left(\frac{r_1}{2}\right)^{1/2}\right] \tag{10}$$

It is possible to further simplify the formula of the van der Waals force to obtain a more practical relation for the case of ($r_2 = r$) as:

$$f_{vdW} = -\frac{\bar{A}(\frac{t}{2})^{1/2}}{8\sqrt{2}(g-2U)^{5/2}} \left[1 - \frac{2(\frac{1+r^{-1}t}{1+0.5r^{-1}t})^{1/2}}{[1+(g-2U)^{-1}t]^{5/2}} + \frac{(1+r^{-1}t)^{1/2}}{[1+2(g-2U)^{-1}t]^{5/2}} \right] \tag{11}$$

Using the appropriate Taylor series expansion and considering $r \ll g$, the obtained relation can be written as:

$$f_{vdW} = -\frac{\bar{A}t^2(\frac{t}{2})^{1/2}}{8\sqrt{2}r^2(g-2U)^{5/2}} \left[\frac{35}{4} \left(\frac{r}{g-2U} \right)^2 - \frac{5}{4} \left(\frac{r}{g-2U} \right) + \frac{3}{16} \right] \approx -\frac{3\bar{A}t^2}{128\sqrt{2}r^{3/2}(g-2U)^{5/2}} \tag{12}$$

2.3 Governing equation

In order to derive the governing equation of the non-tweezers, the minimum energy principle which implies equilibrium when the free energy reaches a minimum value was applied. The elastic potential energy and the work done by molecular and electrical forces can be expressed as (Timoshenko 1987):

$$U_{elas} = \frac{1}{2} \int_0^L E_{eff} I \left[\frac{d^2 U}{dX^2} \right]^2 dX \tag{13-a}$$

$$W_{vdW} = \int_0^L \int_0^U f_{vdW} dU dX \tag{13-b}$$

$$W_e = \int_0^L \int_0^U f_e dU dX \tag{13-c}$$

where U_{elas} , W_{vdW} , and W_e are the elastic energy, the work done by molecular force, and the work done by electrical force, respectively. In above relation, $E_{eff}I$ and X are effective flexural rigidity of each CNT arm and the distant from the clamped end, respectively. By applying minimum energy principle, i.e. $\delta(U-W) = 0$, the following equation is obtained:

$$\begin{aligned} \delta(U - W) &= \delta U_{elas} - \delta W_{vdW} - \delta W_{vdW} \\ &= \int_0^L \left(E_{eff} I \frac{d^2 U}{dX^2} \delta \frac{d^2 U}{dX^2} - f_{vdW} \delta U - f_e \delta U \right) dX \\ &= E_{eff} I \frac{d^2 U}{dX^2} \delta \frac{dU}{dX} \Big|_0^L - E_{eff} I \frac{d^3 U}{dX^3} \delta U \Big|_0^L \\ &\quad + \int_0^L \left(E_{eff} I \frac{d^4 U}{dX^4} - f_{vdW} - f_e \right) \delta U dX = 0 \end{aligned} \tag{14}$$

As there are no deflection and rotation at the fixed end and also due to the absence of bending moment and shear force at the free end of CNT, the boundary value problem for each CNT can be defined as follows:

$$E_{eff} I \frac{d^4 U}{dX^4} = f_{vdW} + f_e \tag{15-a}$$

$$U(0) = \frac{dU}{dX}(0) = 0 \text{ (Geometrical B.C. at fixed end),} \tag{15-b}$$

$$\frac{d^2 U}{dX^2}(L) = \frac{d^3 U}{dX^3}(L) = 0 \text{ (Natural B.C. at free end).} \tag{15-c}$$

By substituting the electrical and van der Waals forces into above relation, the Eq. (15-a) is derived as:

$$E_{eff} I \frac{d^4 U}{dX^4} = \frac{\epsilon_0 \pi V^2}{g \left(1 - \frac{2U}{g} \right) \times \left[\ln \left(\frac{2g}{r} \left(1 - \frac{2U}{g} \right) \right) \right]^2} + \frac{3\bar{A}t^2}{128\sqrt{2}r^{3/2}g^{5/2} \left(1 - \frac{2U}{g} \right)^{5/2}} \tag{16}$$

For simplicity, the variables, governing equation and boundary conditions become dimensionless using relations (17):

$$x = \frac{X}{L}, \tag{17-a}$$

$$u = \frac{U}{g}, \tag{17-b}$$

$$\xi = \frac{2\epsilon_0 \pi V^2 L^4}{E_{eff} I g^2}, \tag{17-c}$$

$$\eta = \frac{6\bar{A}t^2 L^4}{128\sqrt{2}r^{3/2}E_{eff} I g^{7/2}}, \tag{17-d}$$

$$k = \frac{2g}{r}. \tag{17-e}$$

Therefore, the dimensionless form of governing equation of CNT arms is as follow:

$$\frac{d^4 u}{dx^4} = \frac{\xi}{2(1-2u)[\ln(k(1-2u))]^2} + \frac{\eta}{2(1-2u)^{5/2}} \tag{18-a}$$

$$u(0) = \frac{du}{dx}(0) = 0 \text{ (Geometrical B.C. at fixed end),} \tag{18-b}$$

$$\frac{d^2 u}{dx^2}(1) = \frac{d^3 u}{dx^3}(1) = 0 \text{ (Natural B.C. at free end)} \tag{18-c}$$

3 Solution methods

In order to investigate the instability of nano-tweezers, three approaches e.g. applying the Adomian decomposition method (ADM), employing the Homotopy perturbation method (HPM) and using the numerical finite difference solution is utilized in this section. The dimensionless pull-in voltage (ξ_{PI}) i.e. the voltage in which pull-in occurs, and the pull-in deflection (u_{PI}) i.e. the tip deflection of CNT arms where pull-in occurs, are computed via these approaches.

3.1 Homotopy perturbation method (HPM)

The details of use of HPM for solving relation (18) can be found in Appendix A. By using the HPM method, the solution of Eq. (18) can be summarized to:

$$\begin{aligned}
 u(x) = & -A \frac{x^2}{4} - B \frac{x^3}{12} + \left(\frac{\eta}{48} + \frac{\xi}{48 \ln^2(k)} \right) x^4 \\
 & - \left(\frac{\eta}{576} + \frac{\xi}{1440 \ln^2(k)} + \frac{\xi}{720 \ln^3(k)} \right) Ax^6 \\
 & - \left(\frac{\eta}{4032} + \frac{\xi}{10080 \ln^2(k)} + \frac{\xi}{5040 \ln^3(k)} \right) Bx^7 \\
 & + \left[\left(\frac{\eta}{2} + \frac{\xi}{2 \ln^2(k)} \right) \left(\frac{\eta}{16228} + \frac{\xi}{40320 \ln^2(k)} \right. \right. \\
 & + \left. \left. \frac{\xi}{20160 \ln^3(k)} \right) + \left(\frac{\eta A^2}{3072} + \frac{\xi A^2}{4480} \times \left(\frac{1}{3 \ln^2(k)} \right. \right. \right. \\
 & \left. \left. \left. + \frac{1}{\ln^3(k)} + \frac{1}{\ln^4(k)} \right) \right) \right] x^8 + \dots \tag{19}
 \end{aligned}$$

where the constants A and B can be determined by solving the resulting algebraic equation from the B.C at $x = 1$ i.e. using Eq. (18-c). For any given values of η , ξ and k , Eq. (19) can be used to obtain the instability parameters of the nano-tweezers. The instability in Eq. (19) occurs when $d\xi(x = 1)/du \rightarrow 0$. The instability voltage of the system can be determined by plotting the coordinates u vs. ξ .

3.2 Adomian decomposition method (ADM)

The basic idea of the Adomian decomposition method is explained in Momoniat et al. (2007). In this section, ADM is applied to solve the boundary value problem and find the solution in terms of an infinite converged series. The details of the method and mathematical computations are explained in Appendix B. Briefly, the analytical ADM solution of Eq. (18) can be obtained as the following formula:

$$\begin{aligned}
 lu(x) = & -\frac{1}{4} C_1 x^2 - \frac{1}{12} C_2 x^3 + \frac{1}{4!} \left(-\frac{\eta}{2} - \frac{\xi}{2(\ln(k))^2} \right) x^4 \\
 & + \frac{1}{6!} \left(\frac{5\eta}{4} + \frac{\xi}{2(\ln(k))^2} + \frac{2\xi}{2(\ln(k))^3} \right) C_1 x^6 \\
 & + \left(\frac{1}{7!} + \frac{1}{11!} \right) \left(\frac{5\eta}{2} + \frac{\xi}{2(\ln(k))^2} + \frac{\xi}{(\ln(k))^3} \right) C_2 x^7 \\
 & - \frac{1}{8!} \left(\left(\frac{5\eta}{4} + \frac{\xi}{2(\ln(k))^2} + \frac{\xi}{(\ln(k))^3} \right) \right. \\
 & \left. \times \left(\frac{\eta}{2} + \frac{\xi}{2(\ln(k))^2} \right) + \frac{3!}{8!} C_1^2 \right) x^8 + \dots \tag{20}
 \end{aligned}$$

where the constants C_1 and C_2 can be determined by solving the resulting algebraic equation from the B.C at $x = 1$ i.e. using Eq. (18-c). For any given values of η , ξ and k , Eq. (20) can be used to obtain the pull-in parameters of the tweezers. The instability in Eq. (20) occurs when $d\xi(x = 1)/du \rightarrow 0$. The instability parameters of the system can be determined by plotting u vs. ξ .

3.3 Finite difference method (FDM)

In addition to the analytical solutions, a numerical solving procedure based on finite difference method (FDM) is developed in this section (see Appendix C for the details). Following the standard FDM procedure, the beam is discretized into n equal sections (elements) separated by $(n + 1)$ nodes. By discretizing the governing differential equation for each element and incorporating the boundary conditions, an algebraic system of equation is obtained as:

$$[A]\{u\} = \{F\} \tag{21}$$

where $\{u\}$, $\{F\}$ and $[A]$ are displacement vector, force vector and the stiffness matrix, respectively. By numerically solving the algebraic system of equations, the nodal deflections of the CNT arms are computed. When the instability occurs, no solution exists for Eq. (21) and the pull-in parameters of the system can be determined by plotting the CNT tip deflection vs. the applied force.

4 Results and discussion

In this section, first the accuracy of the present model for simulating the instability of nano-tweezers is examined by comparing the theoretical obtained results with the experiments reported in the literature. Afterwards, the obtained results are discussed from the viewpoint of the forces act on the device.

4.1 Comparison with experiment

Kim and Lieber (1999) evaluated the pull-in instability voltage of CNT nano-tweezers with $1\ \mu\text{m}$ initial gap and $45\ \text{nm}$ diameter experimentally. The comparison between the instability voltage which is determined using proposed model and experimental data are presented in Table 1. The experimental results reveal that for a tweezers, the snap down occurs at $8.5\ \text{V}$. Numerical method (FDM) predicts the value of $8.54\ \text{V}$ for snap down voltage of the system. This parameter is analytically computed as 8.27 and $8.75\ \text{V}$ using HPM and ADM, respectively for the mentioned nano-tweezers geometry. As seen, the obtained results show the excellent agreement between the present theoretical model and reported experimental measurements. This reveals the reliability of the present continuum-based model in simulating the static pull-in of the nano-tweezers.

4.2 Tweezers in micro-separations

For micro-scale gap, the Coulomb force is dominant and van der Waals attraction can be neglected due to the large distance between the CNT arms. If the distance between the CNT arms is of the order of few micrometers, the presence of van der Waals force can be neglected. Variation of dimensionless tip deflection of the arms (u_{tip}) versus the voltage parameter (ξ) is presented in Fig. 2 for different k values. Increasing the voltage difference between arms, results in increasing the arms displacement.

When the applied voltage exceeds its critical value, ξ_{PI} , then no solution exists for u_{tip} and the instability occurs. Note that the design of the tweezers is limited by this instability. Figure 2 reveals a good agreement between the analytical and numerical approaches. For example in the case of $k = 1,000$, the difference between the pull-in voltage predicted via analytical methods (e.g. HPM and ADM) and numerical solution (FDM) is $<5\ \%$.

4.2.1 Effect of k value on tweezing range

The geometrical parameter k corresponds to the ratio of gap distance to CNT diameter. The effect of k value on the pull-in parameters of CNT tweezers is demonstrated in Fig. 3.

Table 1 Pull-in voltage obtained from different methods

	FDM	ADM	HPM	Exp. (Kim and Lieber 1999)
Pull in voltage (Volte)	8.54	8.75	8.27	8.5
Difference with experiment (%)	0.45	2.94	2.70	–

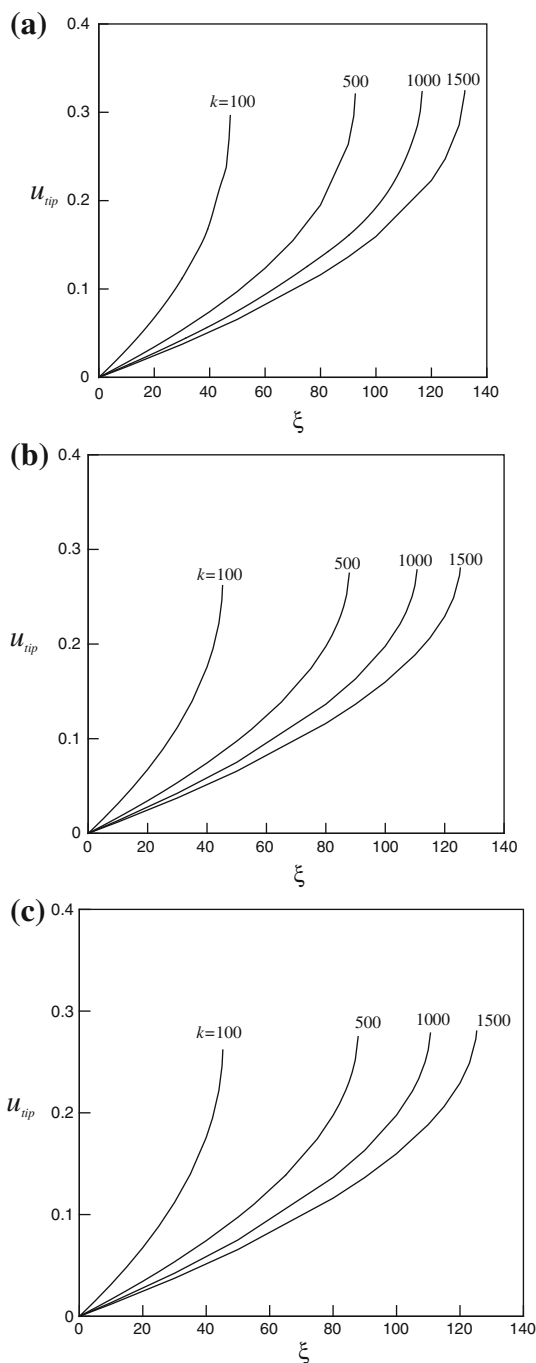


Fig. 2 The variation of tip displacement of arms versus the applied voltage parameter for various k values **a** ADM, **b** HPM, **c** FDM

As shown an increase in k value leads to increase in the ξ_{PI} and u_{PI} of the system. The dependency of u_{PI} on k (Fig. 3b) physically reveals that increasing the arm diameter leads to decreasing the tweezing range due to the higher rigidity of the arms. On the other hand, increasing the gap between the arms, results in increasing the tweezing range of the microsystem. Interestingly, Fig. 3b shows that increase in k does not effectively change the

dimensionless instability deflection (u_{PI}) for $k > 100$. This roughly means decrease in arm diameter does not effectively change the tweezing range if the gap is at least 25 times larger than the arm diameter.

4.3 Freestanding CNT tweezers

Despite micro scales, van der Waals force can highly affect the operation of structure in nano-scales. When the gap between the CNT arms is sufficiently small, then even without an applied voltage, the CNT arms can adhere each other due to the intermolecular attractions. The critical values of van der Waals force, η_C and the corresponding CNT arms critical tip deflection, u_C , can be acquired by setting $\zeta = 0$ and then solving the governing equation of nano-tweezers. For analytical solutions, these critical values can be obtained via plotting $u(x = 1)$ vs. η . Furthermore, for any given η , one can solve the governing equation numerically to obtain the solution $u(x)$.

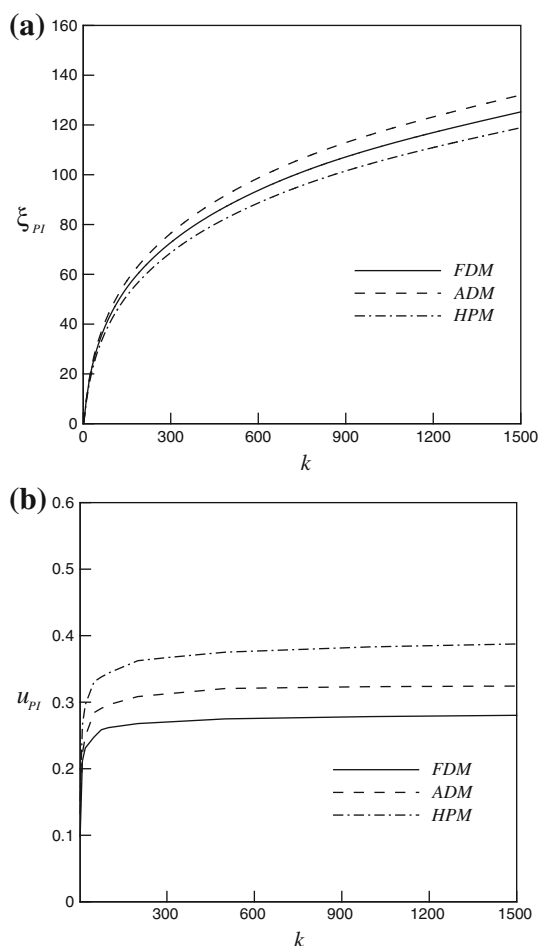


Fig. 3 Effect of k value on the **a** pull-in voltage and **b** pull-in deflection of the CNT tweezers

However, for η greater than critical value of van der Waals attraction, i.e. η_C , stiction occurs and no numerical solution exists.

4.3.1 Detachment length and minimum gap

The relations between van der Waals attraction, η , and the arm’s tip deflection, u_{tip} , are presented in Fig. 4. When η exceeds the critical value η_C , no solution exists for u_{tip} and the stiction occurs. The maximum length of the arms, L_{max} , where the arms do not stick together without the application of a voltage difference is called the detachment length (Ramezani 2011). The detachment length is the maximum permissible length of the freestanding CNT arms. On the other hands, if the length of CNT arms are known, there are a minimum gap, g_{min} , which prevents stiction between the arms due to the van der Waals forces. The maximum length and minimum gap are very important in design CNT tweezers. Substituting η_C into definition of η in Eq. (16-d),

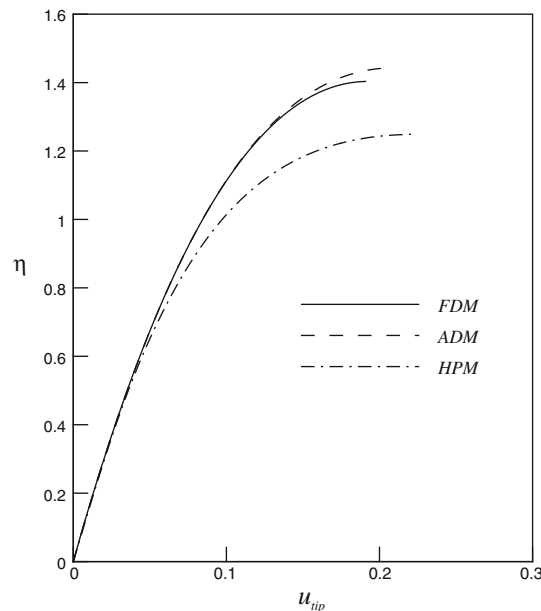


Fig. 4 Relationship between dimensionless molecular force (η) and the CNT arm tip deflections. Stiction occurs when η reaches values greater than η_C

Table 2 Critical value of van der Waals force and corresponding formulas for computing detachment length (L_{max}) and minimum gap (g_{min}) of freestanding CNT tweezers

Method	U_C	η_C	L_{max}	g_{min}
FDM	0.1885	1.403	$2.551 \sqrt[4]{\frac{E_{eff} I g^{7/2} r^{3/2}}{A t^2}}$	$0.343 \sqrt[7]{\frac{A^2 t^4 L^8}{r^3 (E_{eff} I)^2}}$
ADM	0.1887	1.433	$2.564 \sqrt[4]{\frac{E_{eff} I g^{7/2} r^{3/2}}{A t^2}}$	$0.341 \sqrt[7]{\frac{A^2 t^4 L^8}{r^3 (E_{eff} I)^2}}$
HPM	0.2201	1.249	$2.478 \sqrt[4]{\frac{E_{eff} I g^{7/2} r^{3/2}}{A t^2}}$	$0.355 \sqrt[7]{\frac{A^2 t^4 L^8}{r^3 (E_{eff} I)^2}}$

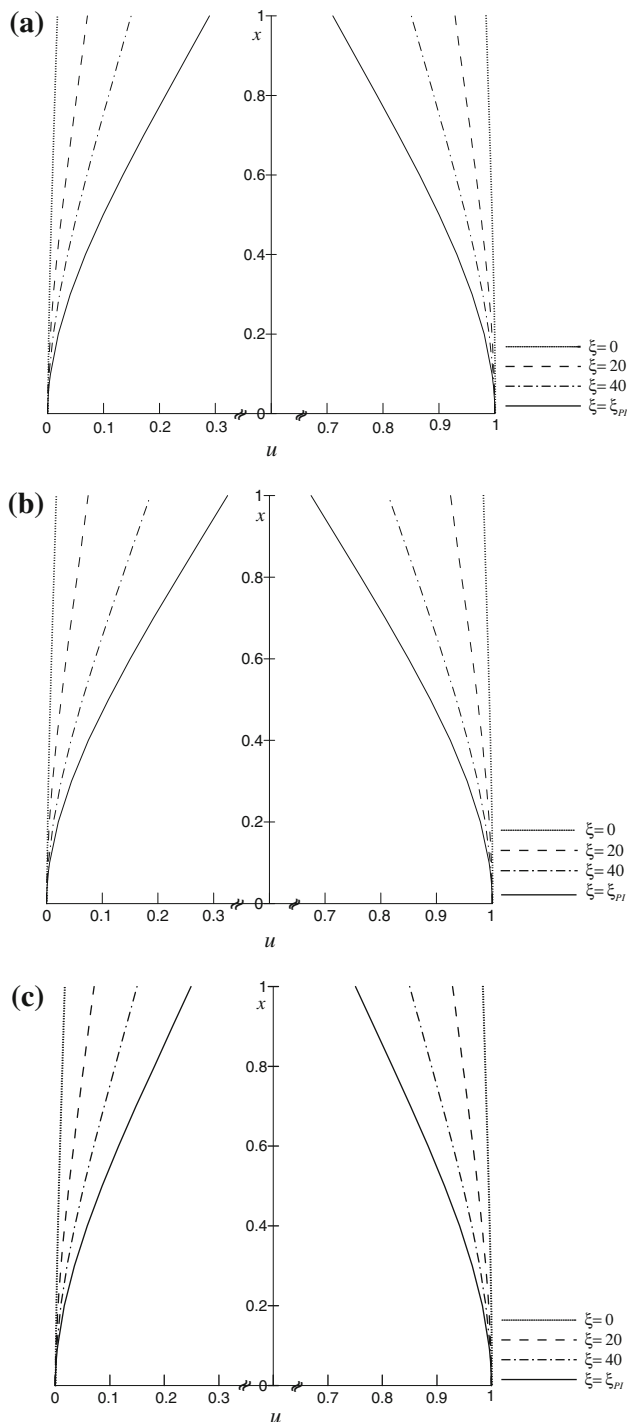


Fig. 5 The variation of the displacements of the micro-tweezers arms for different voltage values (ξ) and considering the van der Waals force ($\eta = 0.5$) **a** ADM, **b** HPM, **c** FDM

we can calculate the values of L_{max} and g_{min} . Table 2 shows the comparison between the L_{max} and g_{min} values obtained by various methods. As shown, the values obtained by analytical solutions are very close to those of numerical solution.

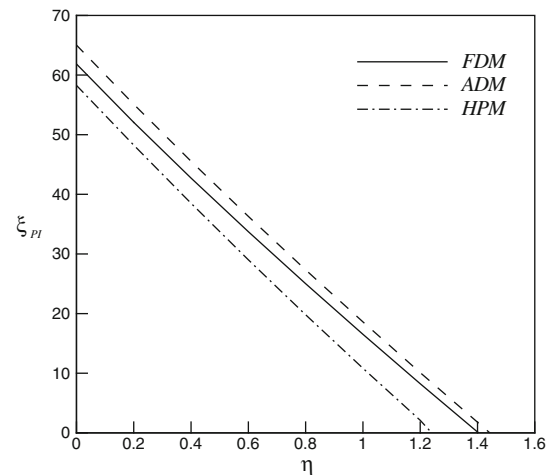


Fig. 6 variation of non-dimensional pull-in voltage (ξ_{PI}) related to non-dimensional intermolecular force (η) for $k = 200$

4.4 Tweezers in nano-separations

In nano-tweezers where the gap between CNT arms are of the order of several nanometers, the combined effects of Coulomb and van der Waals attractions must be taken into account. Figure 5 shows the variation of centerline deflection of each CNT arm for different applied voltage values considering the van der Waals force ($\eta = 0.25$). By increasing the external voltage, the tip displacement is increased until the instability occurs. This figure shows that the nano-tweezers have an initial deflection even when no voltage differential applied. This is due to the presence of molecular force.

The effect of intermolecular force, η , on the pull-in voltage of the nano-tweezers is illustrated in Fig. 6. The obtained results show that by increasing the intermolecular force, the pull-in voltage decrease.

Note that the intersection point of the curves and the horizontal axis corresponds to the critical value of molecular force, η_C . As mentioned in Sect. 4.3, when the CNT arms are enough close together, van der Waals force can induce stiction even without any electrostatic force.

4.4.1 Range of dominancy of van der Waals force

As a case study, typical nano-tweezers fabricated from CNT arms with Young’s modulus of 1 TPa is considered. In this case, I is approximately πtr^3 , where t is typically about 0.35 nm. In order to better understanding the range of dominancy of intermolecular force, we define the correction ratio, CR, as the ratio of ξ_{PI} computed by considering van der Waals force to ξ_{PI} computed by neglecting van der Waals attraction. Figure 7a, b depict the variation of CR as a function of the arm length and initial gap for $r = 1$ nm and $r = 10$ nm, respectively. As shown, this

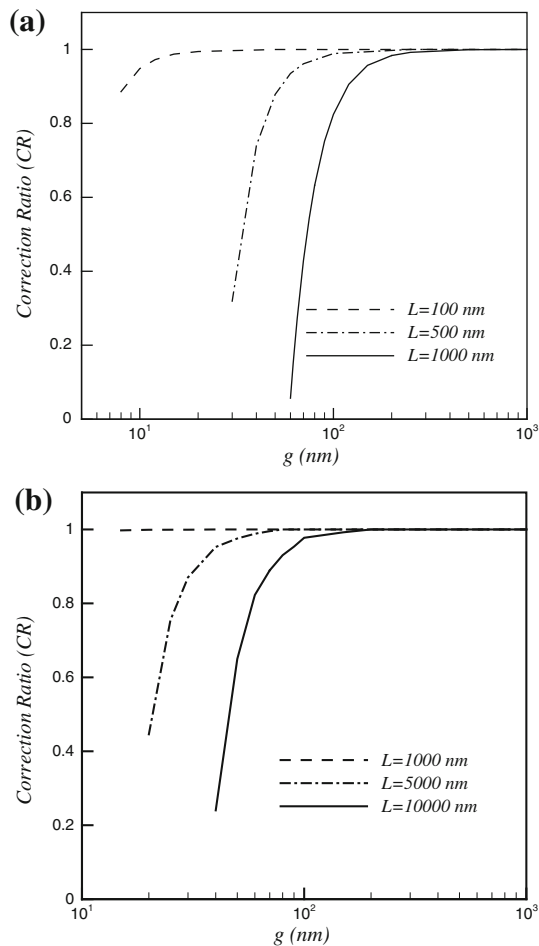


Fig. 7 Variation of correction ratio (CR) for typical CNT tweezers as a function of the arm length and initial gaps: **a** $r = 1$ nm, **b** $r = 10$ nm

case study reveals that effect of intermolecular attraction can be neglected for a wide range of real applications. However, this might produce substantial error in computing the pull-in voltage of the device at separations below 100 nm.

5 Conclusions

In this paper, deflection and instability of CNT tweezers has been studied using a nano-scale continuum model. The developed solutions make parametric studies possible in nano-tweezers design procedures. Results of this study reveals when the applied voltage exceeds its critical value, the instability occurs. It is found that:

1. Increasing the arm diameter leads to decreasing the tweezing range due to the higher rigidity of the arms. Increasing the gap between the arms, results in increasing the tweezing range of the microsystem.

For CNT tweezers with micron-sized gaps (where the van der Waals force is neglected), decrease in arm diameter does not effectively change the tweezing range if the gap is at least 25 times larger than the arm diameter.

2. Results indicate that van der Waals attraction might induce stiction in freestanding CNT tweezers especially at submicron separations even no voltage applied. The proposed model is able to predict the critical values of van der Waals attraction and arm deflection at the onset of the stiction.
3. The maximum stable length of the CNTs and the minimum gap between the CNT arms has been determined for freestanding nano-tweezers. These are fundamental design parameters for preventing the stiction in freestanding nano-tweezers.
4. Presence of the van der Waals force reduces the instability deflection and instability voltage of the CNT tweezers. It is found that the effect of van der Waals force on the pull-in behavior of the nano-tweezers highly depends on the geometrical dimensions of tweezers such as arm length, gap, etc.
5. The influence of intermolecular attraction on instability voltage can be neglected for a wide range of real applications. However, this might produce substantial error in computing the instability voltage at separations below 100 nm.
6. While ADM overestimate the instability voltage in comparison with FDM, the HPM underestimate the pull-in voltage of CNT tweezers. Moreover it is found that the results of the proposed continuum-based model are in a good agreement with the experimental results as reported in the literature.

Appendix A: the homotopy perturbation method (HPM)

In order to solve the Eq. (18), we use the relation $y(x) = 1 - 2u(x)$ to transform the governing equation into the following boundary value problem (21-a):

$$\frac{d^4 y(x)}{dx^4} = -\frac{\xi}{y(x) \ln^2[ky(x)]} - \frac{\eta}{y(x)^{2.5}} \tag{21-a}$$

$$y(0) = 1, y'(0) = 0 \text{ at } x = 0 \tag{21-b}$$

$$y''(1) = 0, y'''(1) = 0, \text{ at } x = 1 \tag{21-c}$$

No exact solution is reported yet for Eq. (21-a) due to high nonlinearity of the problem. In order to obtain an analytical approximation, we can rewrite the boundary value problem (Eq. 21-a) as a system of integral equations using the transformations $dy/dx = p(x)$,

$dw/dx = q(x)$ and $dv/dx = r(x)$ (Abadyan et al. 2011; Koochi et al. 2011a):

$$y(x) = 1 + \int_0^x p(t)dt, \tag{22-a}$$

$$p(x) = 0 + \int_0^x q(t)dt, \tag{22-b}$$

$$q(x) = A + \int_0^x r(t)dt, \tag{22-c}$$

$$r(x) = B - \int_0^x \left(\frac{\eta}{y(x)^{2.5}} + \frac{\xi}{y(x) \ln^2[ky(x)]} \right) dt. \tag{22-d}$$

where A and B are second and third derivative of y with respect to x at $x = 0$, respectively. In order to obtain the solution, we construct the following series (Abadyan et al. 2011; Koochi et al. 2011a):

$$y(x) = \sum_{n=0}^{\infty} s^n y_n(x) \tag{23-a}$$

$$p(x) = \sum_{n=0}^{\infty} s^n p_n(x), \tag{23-b}$$

$$q(x) = \sum_{n=0}^{\infty} s^n q_n(x), \tag{23-c}$$

$$r(x) = \sum_{n=0}^{\infty} s^n r_n(x). \tag{23-d}$$

Using (23) and HPM theory (Abadyan et al. 2011; Koochi et al. 2011a), one can rewrite 22(a–d), in the form of:

$$\sum_{n=0}^{\infty} s^n y_n = 1 + s \int_0^x \left(\sum_{n=0}^{\infty} s^n p_n \right) dt, \tag{24-a}$$

$$\sum_{n=0}^{\infty} s^n p_n = 0 + s \int_0^x \left(\sum_{n=0}^{\infty} s^n q_n \right) dt, \tag{24-b}$$

$$\sum_{k=0}^{\infty} s^n q_n = A + s \int_0^x \left(\sum_{n=0}^{\infty} s^n r_n \right) dt, \tag{24-c}$$

$$\sum_{n=0}^{\infty} s^n r_n = B - s \int_0^x \left(\sum_{n=0}^{\infty} s^n \varphi_n \right) dt. \tag{24-d}$$

The functions φ_n approximate the nonlinear term and are determined via Taylor series expansion (Abadyan et al. 2011; Koochi et al. 2011a):

$$\varphi_n = \frac{1}{n!} \frac{d^n}{ds^n} \left[\sum_{i=0}^{\infty} s^i \left(\frac{\eta}{y_i^{2.5}} + \frac{\xi}{y_i \ln^2[ky_i]} \right) \right]_{s=0} \tag{25}$$

Substituting relation (25) in Eqs. 24(a–d) and comparing the coefficient of like powers of p , we obtain:

$$\begin{aligned} y_0 &= 1, \\ y_1 &= 0, \\ y_2 &= A \frac{x^2}{2}, \\ y_3 &= B \frac{x^3}{6}, \\ y_4 &= - \left(\frac{\eta}{24} + \frac{\xi}{24 \ln^2(k)} \right) x^4, \\ y_5 &= 0, \\ y_6 &= \left(\frac{\eta}{288} + \frac{\xi}{720 \ln^2(k)} + \frac{\xi}{360 \ln^3(k)} \right) Ax^6, \\ y_7 &= \left(\frac{\eta}{2016} + \frac{\xi}{5040 \ln^2(k)} + \frac{\xi}{2520 \ln^3(k)} \right) Bx^7, \\ y_8 &= - \left[\left(\eta + \frac{\xi}{\ln^2(k)} \right) \left(\frac{\eta}{16228} + \frac{\xi}{40320 \ln^2(k)} + \frac{\xi}{20160 \ln^3(k)} \right) \right. \\ &\quad \left. + \left(\frac{\eta}{1536} + \frac{\xi}{6720 \ln^2(k)} + \frac{\xi}{2240 \ln^3(k)} + \frac{\xi}{2240 \ln^4(k)} \right) A^2 \right] x^8, \end{aligned} \tag{26}$$

Appendix B: Adomian decomposition method (ADM)

In order to solve the governing equation of system by analytical ADM, we use the substitution $y(x) = 1 - 2u(x)$, to transform Eq. (18-a) into:

$$\frac{d^4 y(x)}{dx^4} = - \frac{\xi}{y(x) \ln^2[ky(x)]} - \frac{\eta}{y(x)^{2.5}} \tag{27-a}$$

$$y(0) = 1, y'(0) = 0 \text{ at } x = 0 \tag{27-b}$$

$$y''(1) = 0, y'''(1) = 0 \text{ at } x = 1 \tag{27-c}$$

Employing the Adomian decomposition method, the dependent variable in Eq. (27) can be written as

$$y(x) = \sum_{n=0}^{\infty} y_n(x) \tag{28-a}$$

Now consider a fourth-order integral operator $L^{(-4)}$ as:

$$L^{(-4)} = \underbrace{\int_0^x \dots \int_0^x (\cdot) dx \dots dx}_{4\text{-fold}} \tag{28-b}$$

Referring to the Adomian decomposition method from (Tadi Beni et al. 2011; Koochi et al. 2012), the recursive relations of Eq. (B.7) can be provided as

$$\begin{aligned}
 y_0(x) &= 1, \\
 y_1(x) &= \frac{1}{2} C_1 x^2 + \frac{1}{3!} C_2 x^3 + L^{-(4)} [A_0], \\
 y_{n+1}(x) &= L^{-(4)} [A_n].
 \end{aligned}
 \tag{29}$$

where the individual A_n are determined from the following formula:

$$A_n = \frac{1}{n!} \frac{d^n}{d\lambda^n} \left[\sum_{i=0}^n \lambda^i \left(\frac{\eta}{y_i^{2.5}} + \frac{\xi}{y_i \ln^2[ky_i]} \right) \right]_{\lambda=0}.
 \tag{30}$$

Substituting relations (30) in Eq. (29), we obtain the series terms as:

$$\begin{aligned}
 y_0 &= 1 \\
 y_1 &= \frac{1}{2!} C_1 x^2 + \frac{1}{3!} C_2 x^3 - \frac{1}{4!} \left(\eta + \frac{\xi}{\ln^2(k)} \right) x^4 \\
 y_2 &= \frac{1}{6!} \left(2.5\eta + \frac{\xi}{\ln^2(k)} + \frac{2\xi}{\ln^3(k)} \right) C_1 x^6 \\
 &\quad + \frac{1}{7!} \left(2.5\eta + \frac{\xi}{\ln^2(k)} + \frac{2\xi}{\ln^3(k)} \right) C_2 x^7 \\
 &\quad - \frac{1}{8!} \left(\eta + \frac{\xi}{\ln^2(k)} \right) \left(2.5\eta + \frac{\xi}{\ln^2(k)} + \frac{2\xi}{\ln^3(k)} \right) C_2 x^8 \\
 y_3 &= -\frac{1}{8!} \left[26.25\eta + \frac{6\xi}{\ln^2(k)} \left(1 + \frac{3}{\ln(k)} + \frac{3}{\ln^2(k)} \right) \right] C_1^2 x^8 \\
 &\quad - \frac{1}{9!} \left[87.5\eta + \frac{20\xi}{\ln^2(k)} \left(1 + \frac{3}{\ln(k)} + \frac{3}{\ln^2(k)} \right) \right] C_1 C_2 x^9 \\
 &\quad + \frac{1}{10!} \left\{ 30 \left[\left(\eta + \frac{\xi}{\ln^2(k)} \right) C_1 - \frac{C_2^2}{6} \right] \right. \\
 &\quad \times \left[4.375\eta + \frac{\xi}{\ln^2(k)} \left(1 + \frac{3}{\ln(k)} + \frac{3}{\ln^2(k)} \right) \right] \\
 &\quad \left. + \left(2.5\eta + \frac{\xi}{\ln^2(k)} + \frac{2\xi}{\ln^3(k)} \right)^2 C_1 \right\} x^{10} \\
 &\quad + \frac{1}{11!} \left\{ 70 \left(\eta + \frac{\xi}{\ln^2(k)} \right) \right. \\
 &\quad \times \left[4.375\eta + \frac{\xi}{\ln^2(k)} \left(1 + \frac{3}{\ln(k)} + \frac{3}{\ln^2(k)} \right) \right] \\
 &\quad \left. + \left(2.5\eta + \frac{\xi}{\ln^2(k)} + \frac{2\xi}{\ln^3(k)} \right)^2 \right\} C_2 x^{11} \\
 &\quad - \frac{1}{12!} \left\{ \left(\eta + \frac{\xi}{\ln^2(k)} \right) \left(2.5\eta + \frac{\xi}{\ln^2(k)} + \frac{2\xi}{\ln^3(k)} \right) \right\}^2 \\
 &\quad + 840 \left[4.375\eta + \frac{\xi}{\ln^2(k)} \left(1 + \frac{3}{\ln(k)} + \frac{3}{\ln^2(k)} \right) \right] \\
 &\quad \times \left(2.5\eta + \frac{\xi}{\ln^2(k)} + \frac{2\xi}{\ln^3(k)} \right)^2 \Big\} x^{12} \dots
 \end{aligned}
 \tag{31}$$

Appendix C: finite difference method (FDM)

In order to solve the governing equation using FDM, the beam is discretized into n equal elements separated by $n + 1$ nodes. For each element, the governing Eq. (18) in the discretized form can be written as:

$$\frac{u_{i-2} - 4u_{i-1} + 6u_i - 4u_{i+1} + u_{i+2}}{\Delta x^4} = F_i
 \tag{32}$$

where Δx is the grid spacing, u_i is the deflection of i th grid and:

$$F_i = \frac{\xi}{(1 - u_i) \ln^2[k(1 - u_i)]} + \frac{\eta}{(1 - u_i)^4}
 \tag{33}$$

Applying Eq. (32) to all of the elements and incorporating the boundary conditions (Eqs. 18-b and c), a matrix form system of algebraic equations is obtained as:

$$[A]\{u\} = \{F\}
 \tag{34}$$

where $\{u\} = [u_1, u_2, \dots, u_n]^T$, $\{F\} = [F_1, F_2, \dots, F_n]^T$ and A matrix can be defined as:

$$[A] = \begin{bmatrix} 7 & -4 & 1 & 0 & 0 & \dots & 0 & 0 & 0 & 0 \\ -4 & 6 & -4 & 1 & 0 & \dots & 0 & 0 & 0 & 0 \\ 1 & -4 & 6 & -4 & 1 & \dots & 0 & 0 & 0 & 0 \\ 0 & 1 & -4 & 6 & -4 & \dots & 0 & 0 & 0 & 0 \\ 0 & 0 & 1 & -4 & 6 & \dots & 0 & 0 & 0 & 0 \\ 0 & 0 & 0 & 1 & -4 & \dots & 0 & 0 & 0 & 0 \\ \vdots & \vdots & \vdots & \vdots & \vdots & \ddots & \vdots & \vdots & \vdots & \vdots \\ 0 & 0 & 0 & 0 & 0 & \dots & -4 & 6 & -4 & 1 \\ 0 & 0 & 0 & 0 & 0 & \dots & 1 & -4 & 5 & -2 \\ 0 & 0 & 0 & 0 & 0 & \dots & 0 & 1 & -2 & 1 \end{bmatrix}
 \tag{35}$$

By numerically solving the Eq. (34), the nodal deflections that govern the overall deflection of the CNT arms are computed.

References

Abadyan M, Novinzadeh A, Kazemi A (2011) Approximating the effect of the Casimir force on the instability of electrostatic nano-cantilevers. *Phys Scr* 81:015801

Akita S, Nakayama Y (2002) Manipulation of nanomaterial by carbon nanotube nanotweezers in scanning probe microscope. *Jpn J Appl Phys* 41:4242–4245

Baughman RH, Cui CX, Zakhidov AA, Iqbal Z, Barisci JN (1999) Carbon nanotube actuators. *Science* 284:1340–1344

Desquesnes M, Rotkin SV, Alaru NR (2002) Calculation of pull-in voltages for carbon-nanotube-based nanoelectromechanical switches. *Nanotechnology* 13:120–131

- Duan JS, Rach R, Wazwaz AM (2013) Solution of the model of beam-type micro- and nano-scale electrostatic actuators by a new modified Adomian decomposition method for nonlinear boundary value problems. *Int J Non-Linear Mech* 49:159–169
- Girifalco LA, Hodak M, Lee RS (2000) Carbon nanotubes, buckyballs, ropes, and a universal graphitic potential. *Phy Rev B* 62:13104–13110
- Hayt WH (1981) *Engineering electromagnetics*, 4th edn. McGraw-Hill, New York
- Israelachvili JN (1985) *Intermolecular and surface forces with applications to colloidal and biological systems*. Academic, New York
- Jackson JD (1998) *Classical electrodynamics*, 3rd edn. Wiley, New York
- Jiang L, Tan H, Wu J, Huang Y, Hwang K-C (2007) Continuum modelling of interfaces in polymer matrix composites reinforced by carbon nanotubes. *Nano* 2:139–148
- Ke CH, Espinosa HD (2006) Nanoelectromechanical systems (NEMS) and modeling. In: Rieth M, Schommers W (eds) *The Handbook of Theoretical and Computational Nanotechnology*. American Scientific Publishers, Valencia
- Ke CH, Pugno N, Peng B, Espinosa HD (2005) Experiments and modeling of carbon nanotube-based NEMS devices. *J Mech Phys Solids* 53:1314–1333
- Kim P, Lieber CM (1999) Nanotube nanotweezers. *Science* 286:2148–2150
- Kinaret J, Nord T, Viefers S (2003) A carbonnanotube-based nanorelay. *Appl Phy Lett* 82:1287–1289
- Koochi A, Kazemi AS, Abadyan M (2011a) Simulating deflection and determining stable length of freestanding CNT probe/sensor in the vicinity of grapheme layers using a nano-scale continuum model. *NANO* 6:419–429
- Koochi A, Kazemi AS, Noghrehabadi A, Yekrangi A, Abadyan M (2011b) New approach to model the buckling and stable length of multi walled carbon nanotube probes near graphite sheets. *Mater Des* 32:2949–2955
- Koochi A, Noghrehabadi A, Abadyan M, Roohi E (2011c) Investigation of the effect of van der Waals force on the instability of electrostatic Nano-actuators. *Int J Mod Phys B* 25:3965–3976
- Koochi A, Kazemi AS, Khandani F, Abadyan M (2012) Influence of surface effects on size-dependent instability of nano-actuators in the presence of quantum vacuum fluctuations. *Phy Scripta* 85:035804 (7 pp)
- Lee J, Kim S (2005) Manufacture of a nanotweezer using a length controlled CNT arm. *Sens Actuator A* 120:193–198
- Lee SW, Lee DS, Morjan RE, Jhang SH, Sveningsson M, Nerushev OA (2004) A three-terminal carbon nanorelay. *Nano Lett* 4:2027–2030
- Lennard-Jones JE (1930) Perturbation problems in quantum mechanics. *Proc R Soc Lond A* 129:598–615
- Lin WH, Zhao YP (2005) Casimir effect on the pull-in parameters of nanometer switches. *Microsyst Technol* 11:80–85
- Ma JB, Jiang L, Asokanathan SF (2010) Influence of surface effects on the pull-in instability of NEMS electrostatic switches. *Nanotechnology* 21:505–514
- Moeenfard H, Mojahedi M, Ahmadian M (2011) A homotopy perturbation analysis of nonlinear free vibration of Timoshenko microbeams. *J Mech Sci Technol* 25:557–565
- Mojahedi M, Moghimi Zand M, Ahmadian MT, Babaei M (2011) Analytic solutions to the oscillatory behavior and primary resonance of electrostatically actuated microbridges. *Int J Struc Stab Dyn* 11:1119–1137
- Momoniat E, Selway TA, Jina K (2007) Analysis of Adomian decomposition applied to a third-order ordinary differential equation from thin film flow. *Nonlinear Anal Theory Method Appl* 66:2315–2324
- Ramezani A (2011) Stability analysis of electrostatic nanotweezers. *Phys E* 43:1783–1791
- Sasaki N, Toyoda A, Sayito H, Itamura N, Ohyama M, Miura K (2006) Theoretical simulation of atomic-scale peeling of single-walled carbon nanotube from graphite surface. *J Surf Sci Nanotech* 4:133–137
- Sazonova V, Yaish Y, Ustunel H, Roundy D, Arias TA, McEuen PL (2004) A tunable carbon nanotube electromechanical oscillator. *Nature* 431:284–287
- Soroush R, Koochi A, Haddadpour H, Abadyan M, Noghrehabadi A (2010) Investigating the effect of Casimir and van der Waals attractions on the electrostatic pull-in instability of nanoactuators. *Phys Scr* 82:045801 (11 pp)
- Strus MC, Zalamea L, Raman A, Pipes RB, Nguyen CV, Stach EA (2008) Peeling force spectroscopy: exposing the adhesive nanomechanics of one-dimensional nanostructures. *Nano Lett* 8:544–550
- Tadi Beni Y, Koochi A, Abadyan M (2011) Theoretical study of the effect of Casimir force, elastic boundary conditions and size dependency on the pull-in instability of beam-type NEMS. *Phys E* 43:979–988
- Timoshenko S (1987) *Theory of plates and shells*. McGraw Hill, New York
- Wang G-W, Zhang Y, Zhao Y-P, Yang G-T (2004) Pull-in instability study of carbon nanotube tweezers under the influence of van der Waals forces. *J Micromech Microeng* 14:1119–1125
- Zarei O, Rezazadeh G (2008) A novel approach to study of mechanical behavior of NEM actuators using Galerkin method. *Intern J Nanosyst* 1:161–169